Physics and Imaging in Radiation Oncology 16 (2020) 61–68

Contents lists available at ScienceDirect

Physics and Imaging in Radiation Oncology

journal homepage: www.sciencedirect.com/journal/physics-and-imaging-in-radiation-oncology

Original Research Article

# Evaluation of multi-institutional end-to-end testing for post-operative spine stereotactic body radiation therapy

Tomohisa Furuya [a,*], Young K. Lee [b], Ben R. Archibald-Heeren [c], Mikel Byrne [c], Bruno Bosco [c], Jun H. Phua [d], Hidetoshi Shimizu [e], Shimpei Hashimoto [a], Hiroshi Tanaka [e], Arjun Sahgal [b], Katsuyuki Karasawa [a]

[a] Department of Radiology, Tokyo Metropolitan Cancer and Infectious Diseases Center Komagome Hospital, 1138677 Tokyo, Japan
[b] Department of Radiation Oncology, Sunnybrook Odette Cancer Center, University of Toronto, M4N 3M5 Toronto, Ontario, Canada
[c] Radiation Oncology Centres, Sydney Adventist Hospital, Wahroonga, NSW 2076, Australia
[d] Department of Radiation Oncology, National Cancer Center Singapore, 169610 Singapore, Singapore
[e] Department of Radiation Oncology, Aichi Cancer Center Hospital, 4648681 Aichi, Japan

ARTICLE INFO

*Keywords:*
Post-operative spine SBRT
SABR
Impact of metal hardware
End-to-end test
Multi-institutional phantom study

ABSTRACT

*Background and purpose:* Post-operative spine stereotactic body radiation therapy (SBRT) represents a significant challenge as there are many restrictions on beam geometry to avoid metal hardware as it surrounds the target volume. In this study, an international multi-institutional end-to-end test using an in-house spine phantom was developed and executed. The aim was to evaluate the impact of titanium spine hardware on planned and delivered dose for post-operative spine SBRT.

*Materials and methods:* Five centers performed simulation, planning and irradiation of the spine phantom, with/without titanium metal hardware (MB/B), following our pre-specified protocol. The doses were calculated using the centers' treatment planning system (TPS) and measured with radiophotoluminescent glass dosimeters (RPLDs) embedded within each phantom.

*Results:* The dose differences between the RPLD measured and calculated doses in the target region were within ± 5% for both phantoms studied. Differences greater than 5% were observed for the spinal cord and the out-of-the target regions due to steeper dose gradient regions that are created in these plans. Dose measurements within ± 3% were observed between RPLDs that were embedded in MB and B inserts. For the spinal cord and the out-of-target regions surrounded by metal hardware, the dose measured using RPLDs was within 3% different near the titanium screws compared to the dose measured near only the metal rods.

*Conclusion:* We have successfully performed the first multi-institutional end-to-end dose analysis using an in-house phantom built specifically for post-operative spine SBRT. The differences observed between the measured and planned doses in the presence of metal hardware were clinically insignificant.

## 1. Introduction

Patients with spinal metastases could require decompressive surgery and surgical stabilization to reverse neurological deficits, and improve the grade of epidural disease to maximize the effectiveness of post-operative radiation [1–3]. In such patients, post-operative spine stereotactic body radiation therapy (SBRT) might be an optimal therapeutic option aimed at delivering high biologically effective doses to maximize local control [4,5]. However, titanium spinal implants are typically used which could pose problems with respect to the accuracy of the calculated dose which is critical for SBRT.

In order to deliver dose to the targets that surround metal implants, we must identify the shape and density of the metal implants, accurately calculate dose and perform dose delivery with high precision. Different groups have evaluated the impact of metal implants on dose prescription accuracy [6–10]. However, the current literature has not addressed the specific issue of these effects on spine SBRT. Post-operative spine SBRT represents a significant challenge in accurately delivering dose to the

* Corresponding author at: Department of Radiology, Tokyo Metropolitan Cancer and Infectious Diseases Center Komagome Hospital, Honkomagome 18-22, 3-Chome Bunkyo-ku, Tokyo 113-8677, Japan.
*E-mail address:* tfuruya@cick.jp (T. Furuya).

https://doi.org/10.1016/j.phro.2020.09.005
Received 6 May 2020; Received in revised form 18 August 2020; Accepted 22 September 2020
Available online 14 October 2020

target volume as it is not possible to create a beam geometry that completely avoids the metal hardware, given that the target volume surrounds the implants. More specifically, as metal spinal hardware is usually adjacent to the spinal cord, a greater understanding of the dosimetric impact on the spinal cord is needed.

In order to evaluate the dosimetric impact of spine SBRT on the spinal cord in the presence of adjacent metal hardware, we have devised an in-house phantom and executed an end-to-end test which was performed at multiple radiation therapy departments with an established post-operative spine SBRT program.

## 2. Materials and methods

### 2.1. In-house phantom for mailed dosimetry

A phantom with multiple inserts was constructed to simulate a vertebral column with and without titanium rods and screws. The phantom was constructed using an outer acrylic shell and three different anthropomorphic inserts, as described below and illustrated in Fig. 1. The outer phantom was filled with water to simulate tissue. The phantom including inserts with the acrylic shell empty of water was mailed with planning and delivery instructions to all participating centers.

#### 2.1.1. Reference insert

Reference (REF) insert was made up of a water-equivalent solid phantom (Tough Water Phantom WD, Kyoto Kagaku Co., Kyoto, Japan) and aimed to assess an institution's output with basic beam geometry (Fig. 1(b) left). The density was 1.01 g/cm$^3$.

#### 2.1.2. Simply bone insert

The simply bone (B) insert was constructed from tough water, inner and cortical bone-equivalent solid phantom (Tough Inner Bone Phantom, and Tough Cortical Bone Phantom, Kyoto Kagaku Co., Kyoto, Japan) to represent the spinal cord, target bone, and healthy thoracic vertebral bodies respectively. The densities of the inner- and cortical bone-equivalent solid phantom were 1.24 g/cm$^3$, and 1.50 g/cm$^3$, respectively.

#### 2.1.3. Metal-Bone insert

Metal-Bone (MB) insert was constructed similarly to the B insert, with the addition of titanium hardware (Medtronic, Minneapolis, MN, US, see Fig. 1(b) right).

### 2.2. Dosimetry methods

#### 2.2.1. Point dose measurement using radiophotoluminescent glass dosimeters

Radiophotoluminescent glass dosimeters (RPLDs, GD-302 M, Asahi Glass CO., Tokyo, Japan) were used to measure point dose in relevant regions. The diameter and length of the RPLD (and readout region) were 1.5 (1.0) mm and 12 (6) mm, respectively, and the measurable dose range was 0 to 10 Gy. The RPLDs irradiated by each participating center were returned to the study location and converted to absolute dose, similar to the methods described by Mizuno et al. [11], which calibrated the sensitivity of each RPLD and reader. The detail of how the absolute dose was determined is summarized in Supplement 1. The measurement uncertainty of our RPLD system was estimated to be 1.8% with a coverage factor of $k = 2$ for each RPLD. This was estimated considering reproducibility, energy correction, and the phantom correction factor uncertainties [12].

Fig. 1(c) illustrates the holes in the phantom where twenty RPLDs were embedded for measurement. Each insert was constructed to hold twelve RPLDs. The positions of the RPLDs in the MB and B inserts are illustrated in Fig. 1(d) and 1(f). The positions of the RPLDs were designed such that three were placed in different planes of the "target" region and three were placed in different planes of the "out-of-target" region. Within the regions where we expected the spinal cord, where high dose gradient was often observed, two RPLDs were inserted at three different positions. Six RPLDs (#13–18) were used as "control" (i.e. irradiated with a known dose), and the remaining two RPLDs (#19 and #20) were used to check the "background" dose (i.e. not irradiated).

A reference measurement (RPLD #5) was acquired at each centre using REF insert with a field size of $10 \times 10$ cm$^2$ and dose of 6 Gy.

#### 2.2.2. Dose profile measurement using gafchromic films

A dose profile was measured across the gafchromic EBT3 films (ISP, Wayne, NJ, US) that were embedded in the phantom. Two EBT3 films were placed in the axial and sagittal planes through the target and the spinal cord. The profiles were chosen to best represent a line across the center of the spinal cord and two lines across the metal screws. All films were digitized using an Epson GT-X980 flatbed scanner (Epson, Suwa, Japan) with a resolution of 72 dpi and analyzed using the red channel (16 bit). The optical density (OD) value of the film was converted to dose using an OD-dose calibration table specific to the EBT3 film and scanner used. RPLD #5, located close to the central axis, was used to normalize the film dose distributions. SNC Patient software (Sun Nuclear Corp., Melbourne, FL, US) was used to obtain the film dose distributions.

### 2.3. Treatment planning and delivery

A computed tomography (CT) scan of the MB phantom was acquired and an SBRT was planned following the center's specific spine SBRT planning workflow (Figure S1). "Contour and planning objectives list" (Table S1) accompanied the phantom to provide consistent contour names, prescription dose and organs-at-risk (OAR) constraints for planning.

Planning doses to those in practice at the University of Toronto [1] were linearly scaled in order to deliver dose within the limitation of RPLD dosimetric range. Dose to the 0.035 cm$^3$ of spinal cord planning organ at risk volume ($PRV_{cord}$; spinal cord plus a 2-mm uniform expansion) was constrained to a dose proportional to 17 Gy [13].

The plan created on MB phantom was transferred and recalculated on the CT scan of the B phantom. The two plans were then delivered to the phantom with corresponding inserts. The doses measured by RPLD and EBT3 film were inclusive of all imaging and planned doses. Imaging doses were considered negligible and not accounted for in the planned dose in this study.

### 2.4. Participating institution information

Five academic institutions with established post-operative spine SBRT programs (from Singapore, Australia, Canada and two centers from Japan) participated in this study. Table S2 summarizes information on the treatment planning system (TPS), machine and technique utilized for spine SBRT at each institution. All centres used either a step-and-shoot intensity modulated radiation therapy (IMRT) or a volumetric modulated arc therapy technique using a linac with cone-beam CT image guidance. All treatment plans were calculated with a Monte Carlo (dose to medium) or convolution/superposition technique with heterogeneity corrections and used a $\leq 2.5$ mm grid resolution.

Titanium hardware and CT artifacts caused by the presence of high density material were accounted for according to institution protocol. Institution A used a dual energy CT (SOMATOM Definition Flash, Siemens, Forchheim, Germany) as a secondary image acquisition, which provided a method to reduce metal artifacts from beam hardening. The delineated hardware was assigned an electron density of titanium, and its artifacts were defined as water. Institution B used CT images with the algorithm interactive metal artifact reduction (iMAR) to calculate dose. iMAR, developed by Siemens, is based on frequency split MAR, which enhances the visibility of fine details. Institution B assigned the titanium hardware to its electron density. Institutions C and D separated the hardware and artifacts semi-automatically using uncorrected CT images.

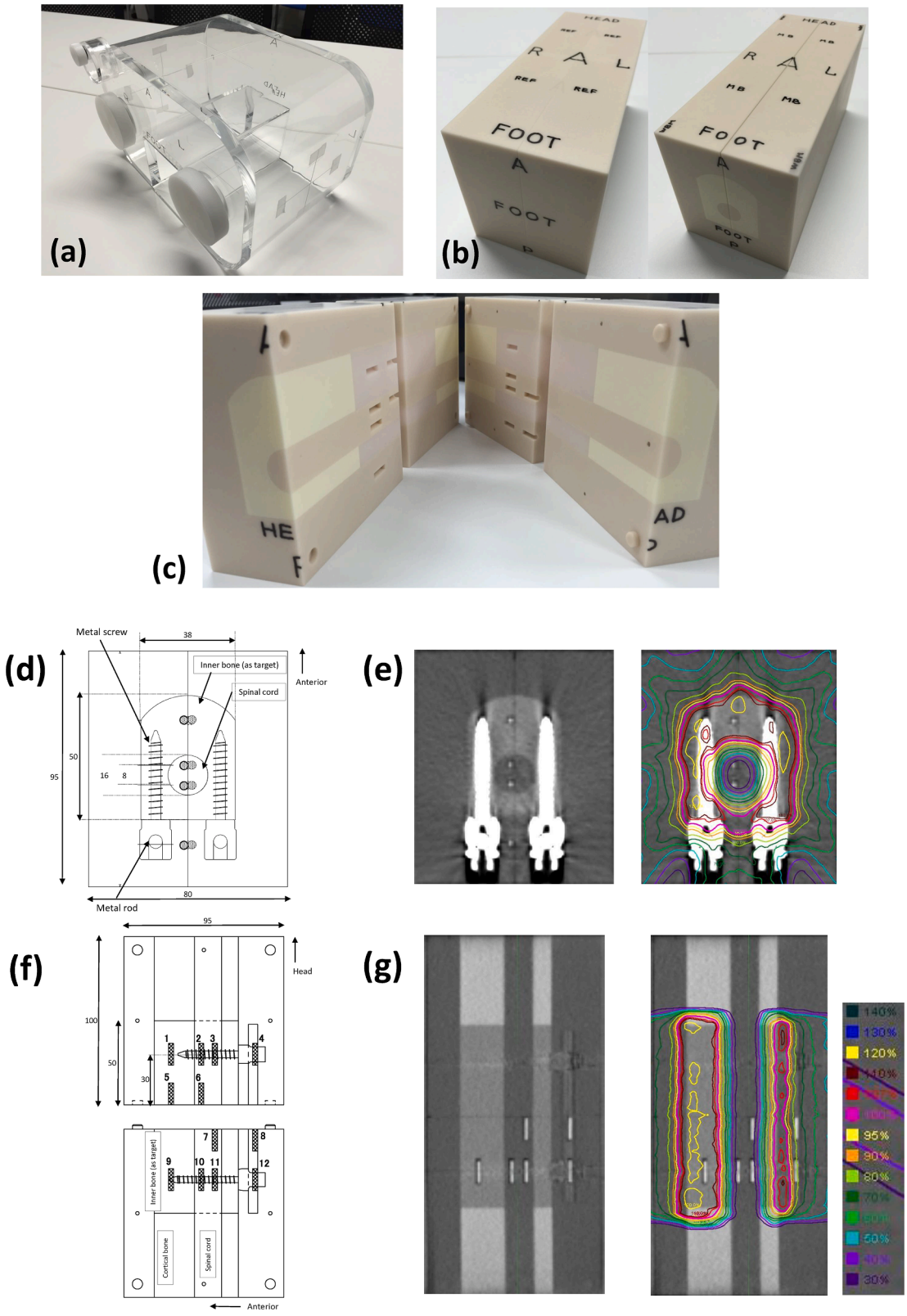


**Fig. 1.** (a-c) Photograph of our in-house spine phantom. (a) the anthropomorphic outer acrylic shell which was filled with water for the study, (b) (left) reference insert, (right) Metal-Bone "MB" (or only Bone "B") inserts, (c) internal structure of the MB insert. All inserts had twelve holes that could house radiophotoluminescent glass dosimeter (RPLD) and could place two films into axial and sagittal planes through the center of target (pink). (d-g) A schematic of the MB insert shown in two different views (d) axial, (f) sagittal and its computed tomography images (e) axial and (g) sagittal with the representative dose distributions shown on the right. In (d), the positions of RPLDs were shown as circles. (f) the sagittal plane through metal screws. The positions of RPLD were shown using rectangles. The dimensions were shown in millimeters. (For interpretation of the references to colour in this figure legend, the reader is referred to the web version of this article.)

The two centres assigned the physical densities of titanium and water to the hardware and artifact contours respectively. Institution E delineated titanium hardware and the artifacts semi-automatically and assigned a physical density of water to these contours.

### 2.5. Data analysis

All DICOM-RT files (CT, STRUCT, PLAN, DOSE for phantoms with MB and B inserts) from each institution were imported into MIM version 6.2.6 (MIM software, Cleveland, OH, USA) at the study center. The RPLD readout regions were delineated using the CTs and the mean calculated dose to each RPLD was extracted from the plan. $D_{MB}^{TPS}$, and $D_{B}^{TPS}$ denoted the mean doses calculated by TPS and $D_{MB}^{RPLD}$, and $D_{B}^{RPLD}$ were the measured doses using RPLDs for the phantoms with MB and B inserts respectively.

Four different evaluations were performed as follows:

1) Accuracy of beam delivery was evaluated by comparing the calculated and measured doses in the presence of titanium hardware. The ratio of $D_{MB}^{RPLD}$ to $D_{MB}^{TPS}$ ($D_{MB}^{RPLD}/D_{MB}^{TPS}$) was compared with the ratio of $D_{B}^{RPLD}$ to $D_{B}^{TPS}$ ($D_{B}^{RPLD}/D_{B}^{TPS}$). For RPLDs in the "target" and "out-of-target" volumes, each measurement point was compared, and for the dose to the "spinal cord" region the average of the two RPLDs located in the same plane was studied. The maximum distance-to-agreement (DTA) for 4.2 Gy (the proportional dose constraint for the $PRV_{cord}$) between the calculated and EBT3 film measurement was used to evaluate the calculation accuracy in the dose-fall-off region.
2) The ratio of the $D_{MB}^{RPLD}$ to the $D_{B}^{RPLD}$ ($D_{MB}^{RPLD}/D_{B}^{RPLD}$) was used to evaluate how much perturbation was introduced by the presence of the metal.
3) The impact of metal hardware (titanium rods and screws) on the maximum point dose ($D_{max}$) of the "spinal cord" region was studied by $D_{max}$ points calculated on the three different axial planes through the "target" region when hardware was present. The point $D_{max}$ was compared between the plans on phantom with MB and B inserts.
4) Dose-volume statistics were studied and compared to $D_{MB}^{RPLD}$ and $D_{MB}^{TPS}$ in both "target" and OAR regions. The specific dose-volume metrics studied were total dose to 99%, 95%, 50%, 2% volumes ($D_{99}$, $D_{95}$, $D_{50}$, and $D_{2}$), and mean dose ($D_{mean}$) to the planning target volume ($PTV_{evl}$, defined as PTV excluding the $PRV_{cord}$). The total doses to 5.0, 1.0, and 0.035 $cm^3$ ($D_{5cc}$, $D_{1cc}$, and $D_{0.035cc}$,) of the spinal cord were selected and compared with the $D_{MB}^{RPLD}$, $D_{MB}^{TPS}$ in each region. Specifically, the relationship between the value of $D_{0.035cc}$ of the spinal cord and $D_{MB}^{RPLD}$ was studied as the maximum dose to the spinal cord can be used as a predictor of radiation myelopathy [13–16].

## 3. Results

In all institutions, the measured dose under the reference conditions agreed with each reported dose to within 3%. All centers produced spine SBRT plans on the MB phantom that satisfied the specified objectives as shown in Table S1. Fig. 1(e) and 1(g) showed CT images and a typical axial and sagittal dose distributions. The RPLDs in the "out-of-target" volume and spinal cord were located close to the field edge and at the steep dose gradient region. The total volume of titanium hardware was defined as 14.3 $cm^3$ (A), 23.7 $cm^3$ (B), 15.0 $cm^3$(C) and 12.9 $cm^3$ (D). Institution E did not distinguish between the titanium hardware and its artifacts.

Fig. 2 summarizes the data on dose perturbation evaluation. The data from different centers showed differences in the calculated to measured dose with and without the presence of the titanium hardware. For the target, the difference in all $D_{MB}^{RPLD}$ and $D_{MB}^{TPS}$ were within ± 5%. For the spinal cord and the out-of-the target volume, larger differences between $D_{MB}^{RPLD}$ and $D_{MB}^{TPS}$ were observed for three centers, however, for centers C and D the differences were < 5%. Similar findings were observed between $D_{B}^{RPLD}$ and $D_{B}^{TPS}$. For E, measured dose was much higher than calculated dose in spinal cord region.

All differences between $D_{MB}^{RPLD}$ and $D_{B}^{RPLD}$ (Fig. 2 right) were within ± 3%, except for a section in the out-of-target and spinal cord region. These regions that presented a larger difference (RPLD #2, 3, 10, 11 in the spinal cord, and #4, 12 in the out-of-target regions) were adjacent to the titanium screws (Fig. 1(d)). Note that the dose difference between $D_{MB}^{RPLD}$ and $D_{B}^{RPLD}$ tended to be larger in these regions than those compared in the absence of the titanium screws (existence of rods only). In the region of spinal cord, the median (range) difference was 1.7 (0.1 – 9.2)%. In the region of "out-of-target", the median (range) difference was 2.5 (1.0 – 5.5)%. In the target, for the RPLDs that were not embedded between the metal screws, the median (range) difference was 0.5 (0.1 – 1.1)%. The EBT3 measurement data compared well with calculated profiles (Fig. 3) and this was consistent from all institutions. The maximum dose profile displacement (4.2 Gy in the spinal cord) was within 2 mm.

The maximum calculated dose to the spinal cord on a plane through the center of the target region and two planes between the metal screws in the phantom, with the MB insert and those at the same positions in the B insert are summarized in Table 1. For institutions A, B and C, where metal hardware was delineated and assigned titanium density, the maximum dose within the spinal cord region between the metal screws was 0.14 Gy lower than that measured with the B insert. However, for Institution E, in which the metal hardware was delineated and overridden to water, the calculated dose difference between the phantoms

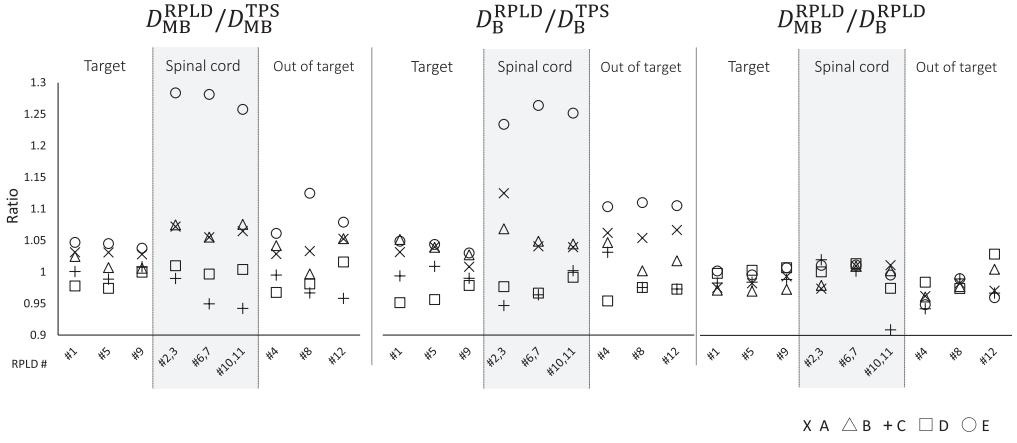


**Fig. 2.** Ratio of RPLD measurement and the calculated doses by treatment planning system (TPS). $D_{MB}^{TPS}$, and $D_{B}^{TPS}$ were the doses calculated by TPS for metal-bone (MB) and bone (B) phantoms, respectively, and $D_{MB}^{RPLD}$, and $D_{B}^{RPLD}$ were the doses measured using RPLDs for the MB and B phantoms, respectively. The legend for the matching shapes to letters indicated results from the different institutions.

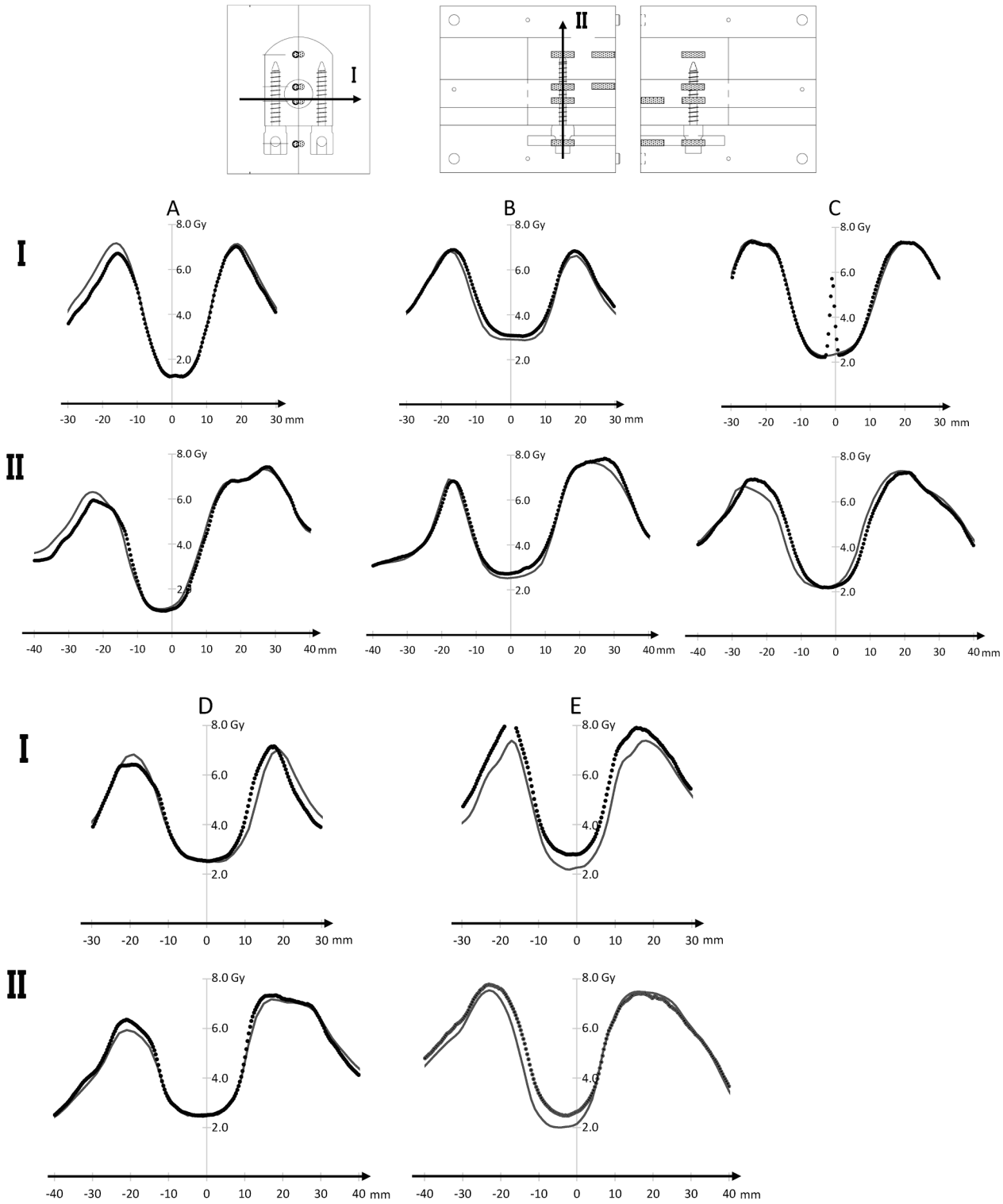


**Fig. 3.** Plots of dose profiles taken from scanned films from Institutions A to E. (I) right-left profiles taken from an axial film. (II) Posterior-anterior profiles taken from a sagittal film. Each gray line was the calculated dose profile taken from DICOM dose file. The center spike of the dose profile I in Institution C was due to a crack in the film.

was negligible. Fig. 4 summarizes the major DVH metrics studied. $PTV_{evl}$ $D_{MB}^{RPLD}$ and $D_{MB}^{TPS}$ were higher than $D_{99}$, and 6 Gy, the proportional prescription dose. In terms of the spinal cord, for Institutions A to D, we observed that both $D_{MB}^{RPLD}$ and $D_{MB}^{TPS}$ did not exceed $D_{0.035cc}$ of the spinal cord. However for Institution E, a 25% difference was observed between $D_{MB}^{RPLD}$ and $D_{MB}^{TPS}$ (see Fig. 2), and one of the $D_{MB}^{RPLD}$ was higher than their spinal cord $D_{0.035cc}$.

## 4. Discussion

Specifically for spine SBRT, it is critical to minimize dose delivery prediction uncertainty caused by the presence of metal hardware. This

**Table 1**
Calculated maximum point dose of spinal cord on three different axial planes for each phantom.

| Institution | Position of axial plane | $D_{max}$ (Gy) of spinal cord calculated in (i) Metal phantom | (ii) Bone phantom | (i) – (ii) (Gy) |
|---|---|---|---|---|
| A | Center of target | 3.02 | 3.08 | −0.06 |
| | Metal hardware (Cranial) | 3.15 | 3.29 | −0.14 |
| | Metal hardware (Caudal) | 3.30 | 3.50 | −0.20 |
| B | Center of target | 3.31 | 3.31 | 0 |
| | Metal hardware (Cranial) | 3.08 | 3.20 | −0.12 |
| | Metal hardware (Caudal) | 3.13 | 3.26 | −0.13 |
| C | Center of target | 2.93 | 2.92 | 0.01 |
| | Metal hardware (Cranial) | 3.01 | 3.12 | −0.11 |
| | Metal hardware (Caudal) | 2.93 | 3.10 | −0.17 |
| E | Center of target | 3.36 | 3.35 | 0.01 |
| | Metal hardware (Cranial) | 3.26 | 3.28 | −0.02 |
| | Metal hardware (Caudal) | 3.36 | 3.42 | −0.06 |

Institution D submitted only the values of TPS-calculated point doses for RPLD in the Bone phantom. Therefore, those data were excluded from this table. *Abbreviations*: $D_{max}$ = Maximum point dose.

multi-institutional end-to-end dose analysis, with a spine anthropomorphic phantom using RPLDs and films, evaluated the impact of metal hardware on the dose calculation results. Different clinical planning strategies and beam deliveries from multiple centers that treat spine SBRT were compared using the same phantom.

Previously published studies on the impact of spinal metal hardware on the dose calculation, and the beam delivery specific to spine SBRT using IMRT techniques [17–19] have been limited. For example, Son et al. investigated the effects of titanium spinal implants on the dose calculated by the TPS for various delivery techniques such as ARTISTE, TomoTherapy and CyberKnife using three different types of imaging namely kVCT, extended kVCT and MVCT with an in-house homogeneous phantom with/without the titanium pedicle screws [17]. The difference between the planning dose and the measured dose in the space between the metal screws, using a CC01 (0.01 cc) ionization chamber, was reported to be within ± 3%. However, their study only compared one point dose measurement at the center of a circular-shaped target. Furthermore, the plan that was compared was a simple plan as opposed to a highly complex spine SBRT plan. Cheng et al. also evaluated the dose prediction accuracy near titanium hardware for spine SBRT using immersed gafchromic films embedded within an in-house water phantom with titanium spinal hardware [19]. A comparison between the measured and calculated doses for a simple plan with six open-fields was performed, and showed greater than 95% agreement with a gamma criterion of 2%/2mm for the commercial TPS dose calculation algorithms. They suggested that these results were due to the averaging effects of the multiple inter-modulated beams, and concluded that the accuracy of the dose calculation was clinically acceptable in spine SBRT. However, they only reported the relative dose analysis using film and data were acquired utilizing only a uniform density water phantom. Huang et al. reported approaches to reducing TPS dose calculation errors near metal implants using an in-house spine phantom with ion chamber measurements [20]. In their study, the comparison of the TPS dose calculation errors with and without titanium rods was performed, and they reported negligible differences (<1.0%) using uncorrected imaging methods. They also investigated the dosimetric impact of several commercial CT MAR methods in detail, and concluded that the studied artifact reduction methods did not have a large, or even positive effect on dose calculation accuracy. Our study was specific to dose calculation differences in the presence and absence of titanium hardware for post-operative spine SBRT, and confirms aspects of Huang's report [20]. We also present a more clinically relevant spine SBRT planning study by performing an inter-comparison with a collection of multi-institutional end-to-end test data using a realistic in-house spine phantom. The design of the phantom was such that not only we are able to study the effect of titanium rods and titanium screws on the spinal canal region, but also the calculation issues that could be present when hardware densities are not accounted for in the dose calculations.

With regard to the definition of hardware, it should be noted that the volumes of the delineated titanium hardware in Institutions A and B were substantially different, though both centers utilized CT MAR techniques. Furthermore, the titanium hardware volume identified by Institution A was similar to those of the institutions using uncorrected CT images. This variation was most probably due to the window level and width differences in delineating the metal hardware, which

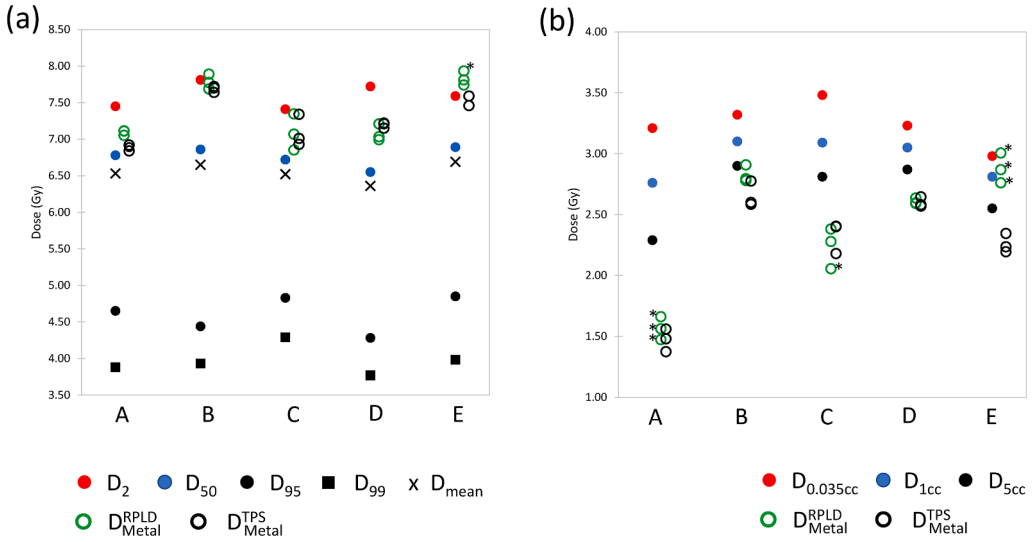


**Fig. 4.** Plots of dose-volume-histogram metrics of $D_{99}$, $D_{95}$, $D_{50}$, $D_2$ and the mean dose ($D_{mean}$) for $PTV_{evl}$ (a) and $D_{5cc}$, $D_{1cc}$, and $D_{0.035cc}$ for spinal cord (b) in Metal phantom plan by institutions A to E. $D_X$ meant the total dose to X% (or cc) of each volume. The point measured- ($D^{RPLD}_{Metal}$), calculated-dose ($D^{TPS}_{Metal}$) was also plotted in (a) and (b). * showed the point measured doses with different greater than 5% from the calculated doses.

highlights the challenge in correctly defining the shape of metal implants in RT planning.

In this study, we also addressed four specific aspects of planning post-operative spine SBRT in the presence of titanium hardware and conclude: 1) Regardless of the presence of the titanium hardware, the degree of the dose calculation differences was different among the three regions studied; target, spinal cord and out-of-target. A possible reason for this observation was the RPLD measurement uncertainty being greater for very steep dose gradient regions, and not due to the accuracy of the dose calculations. Molineu et al. also reported a similar reasoning in the differences observed using TLDs when studying the region between the OAR and PTV for head-and-neck IMRT [21]; 2) Dose perturbation introduced by the presence of metal was studied with the difference observed between $D_{MB}^{RPLD}$ and $D_{B}^{RPLD}$, which was within 3% in the target and the spinal cord. This small difference indicates that the impact of titanium hardware on dose delivery is in a clinically acceptable range. This result is consistent with Huang et al.'s study [20]. Although these differences were small, a larger dataset would be required to reduce uncertainties in the phantom setup; 3) Our results from regions tested near the hardware (Table 1) showed that the dose calculation with the metal hardware density assignment did impact on our results for the calculated $D_{max}$ of the spinal cord, especially at the region near the metal screws. This observation has not been previously reported. However, we must note that our dataset was limited and a larger investigation would be required to confirm our results and reduce the uncertainty; 4) Point dose calculation differences greater than 5% (the point with an asterisk shown in Fig. 4) should be a concern in spine SBRT. However, target $D_{MB}^{RPLD}$ and $D_{MB}^{TPS}$ that were measured to be higher than $D_{99}$, and the prescription dose were considered clinically acceptable with spine SBRT as we try to maximize the PTV receiving the prescription dose. Similarly, if the measured RPLD dose was sufficiently lower than the spinal cord $D_{max}$, this difference could be considered clinically negligible. However, a substantial dose calculation difference where the measured dose was larger in the spinal cord region, as observed from Institution E (greater than25%), would not be acceptable because the measured dose was larger than $D_{0.035cc}$ of the spinal cord. This particular difference points to a beam modelling discrepancy. We asked Institution E to confirm the large beam delivery difference for the spinal cord using their customary quality assurance tools, and they confirmed this error by measurements with a two-dimensional diode array detector.

It should be noted that the delivery of these plans could be more challenging than clinical plans as leaf motion and gantry speed would increase due to the halving of the prescription dose. To address this concern, the study institution confirmed the integrity of plan delivery with a three-dimensional diode array detector on a test "halved" plan. The results showed a pass rate of gamma analysis of 93.2% with the criteria of 3% dose difference and a 2 mm distance-to-agreement. Therefore, we concluded that the increased speed of the leaves and gantry caused by halving the dose likely yields negligible impact on beam delivery. We also acknowledge that our phantom study does not simulate a post-operative patient with spinal metastases perfectly, and in some situations the spinal cord position *in vivo* might be closer or further away from the hardware which may limit the generalizability of these observations.

We conclude that when density corrections are applied and adequate dose calculation algorithms used, there is a small clinical impact on the dose delivered to the target and the spinal cord regions in the presence of metal hardware. However, care should be taken with regard to the proximal region between metal hardware and the spinal cord.

## 5. Responsible for statistical analyses

Tomohisa Furuya was responsible for them.

## 6. Summary

This multi-institutional phantom study evaluated the impact of metal hardware on the accuracy of dose calculation specific to post-operative spine stereotactic body radiation therapy (SBRT), given that accurate evaluation of dose in this scenario is critical. A phantom was created with multiple inserts and circulated to five international centers. We have shown that the dose to the target could be calculated within ± 5% despite the presence of metal hardware adjacent to the spinal metastases target volume.

## Declaration of Competing Interest

The authors declare the following financial interests/personal relationships which may be considered as potential competing interests: Dr. Arjun Sahgal has received honorarium for past educational seminars from Medtronic and Elekta AB and research grants from Elekta AB.

Dr. Arjun Sahgal has participated on the medical advisory board for Varian Medical Systems and Merck.

Dr. Arjun Sahgal has received honorarium for past educational seminars from Accuray and Medtronic.

*Acknowledgements*

A development of our phantom was supported by Clinical Research Fund of Tokyo Metropolitan Government. We acknowledge the technical support of Taisei Medical Company.

*Source of Financial Support/Funding Statement*

A development of our phantom was supported by Clinical Research Fund of Tokyo Metropolitan Government.

## Appendix A. Supplementary data

Supplementary data to this article can be found online at https://doi.org/10.1016/j.phro.2020.09.005.

## References

[1] Tseng CL, Soliman H, Myrehaug S, Lee YK, Ruschin M, Atenafu E, et al. Imaging-Based Outcomes for 24 Gy in 2 Daily Fractions for Patients with de Novo Spinal Metastases Treated With Spine Stereotactic Body Radiation Therapy (SBRT). Int J Radiat Oncol Biol Phys 2018;102:499–507.

[2] Jakubovic R, Ruschin M, Tseng CL, Pejovic-Milic A, Sahgal A, Yang VXD. Surgical Resection With Radiation Treatment Planning of Spinal Tumors. Neurosurgery 2018;84:1242–50.

[3] Al-Omair A, Masucci L, Masson-Cote L, Campbell M, Atenafu EG, Parent A, et al. Surgical resection of epidural disease improves local control following postoperative spine stereotactic body radiotherapy. Neuro Oncol 2013;15:1413–9.

[4] Sahgal A, Bilsky M, Chang EL, Ma L, Yamada Y, Rhines LD, et al. Stereotactic body radiotherapy for spinal metastases: current status, with a focus on its application in the postoperative patient: a review. J Neurosurg-Spine 2011;14:151–66.

[5] Redmond KJ, Lo SS, Fisher C, Sahgal A. Postoperative stereotactic body radiation therapy (SBRT) for spine metastases: a critical review to guide practice. Int J Radiat Oncol Biol Phys 2016;95:1414–28.

[6] Keall PJ, Siebers JV, Jeraj R, Mohan R. Radiotherapy dose calculations in the presence of hip prostheses. Med Dosim 2003;28:107–12.

[7] Bazalova M, Beaulieu L, Palefsky S, Verhaegen F. Correction of CT artifacts and its influence on Monte Carlo dose calculations. Med Phys 2007;34:2119–32.

[8] Kim Y, Tomé WA, Bal M, McNutt TR, Spies L. The impact of dental metal artifacts on head and neck IMRT dose distributions. Radiother Oncol 2006;79:198–202.

[9] Spadea MF, Verburg JM, Baroni G, Seco J. The impact of low-Z and high-Z metal implants in IMRT: a Monte Carlo study of dose inaccuracies in commercial dose algorithms. Med Phys 2014;41.

[10] Kamomae T, Itoh Y, Okudaira K, Nakaya T, Tomida M, Miyake Y, et al. Dosimetric impact of dental metallic crown on intensity-modulated radiotherapy and volumetric-modulated arc therapy for head and neck cancer. J Appl Clin Med Phys 2016;17:234–45.

[11] Mizuno H, Kanai T, Kusano Y, Ko S, Ono M, Fukumura A, et al. Feasibility study of glass dosimeter postal dosimetry audit of high-energy radiotherapy photon beams. Radiother Oncol 2008;86:258–63.

[12] Mizuno H, Fukumura A, Fukahori M, Sakata S, Yamashita W, Takase N, et al. Application of a radiophotoluminescent glass dosimeter to nonreference condition dosimetry in the postal dose audit system. Med Phys 2014;41:112–1104.
[13] Sahgal A, Weinberg V, Ma L, Chang E, Chao S, Muacevic A, et al. Probabilities of radiation myelopathy specific to stereotactic body radiation therapy to guide safe practice. Int J Radiat Oncol Biol Phys 2013;85:341–7.
[14] Sahgal A, Ma L, Gibbs I, Gerszten PC, Ryu S, Soltys S, et al. Spinal cord tolerance for stereotactic body radiotherapy. Int J Radiat Oncol Biol Phys 2010;77:548–53.
[15] Sahgal A, Ma L, Weinberg V, Gibbs I, Chao S, Chang UK, et al. Reirradiation human spinal cord tolerance for stereotactic body radiotherapy. Int J Radiat Oncol Biol Phys 2012;82:107–16.
[16] Sahgal A, Chang JH, Ma L, Marks LB, Milano MT, Medin P, et al. Spinal cord dose tolerance to stereotactic body radiation therapy. Int J Radiat Oncol Biol Phys 2019; 139:S95–6.
[17] Son SH, Kang YN, Ryu MR. The effect of metallic implants on radiation therapy in spinal tumor patients with metallic spinal implants. Med Dosim 2012;37:98–107.
[18] Wang X, Yang JN, Li X, Tailor R, Vassilliev O, Brown P, et al. Effect of spine hardware on small spinal stereotactic radiosurgery dosimetry. Phys Med Biol 2013; 58:6733–47.
[19] Cheng ZJ, Bromley RM, Oborn B, Carolan M, Booth JT. On the accuracy of dose prediction near metal fixation devices for spine SBRT. J Appl Clin Med Phys 2016; 17:5536.
[20] Huang JY, Followill DS, Howell RM, Liu X, Mirkovic D, Stingo FC, et al. Approaches to reducing photon dose calculation errors near metal implants. Med Phys 2016;43:5117–30.
[21] Molineu A, Followill DS, Balter PA, Hanson WF, Gillin M, Huq MS, et al. Design and implementation of an anthropomorphic quality assurance phantom for intensity-modulated radiation therapy for the Radiation Therapy Oncology Group. Int J Radiat Oncol Biol Phys 2005;63:577–83.